Explore 21 (2025) 103232

Contents lists available at ScienceDirect

EXPLORE

journal homepage: www.elsevier.com/locate/jsch

Original Research

Protective effect of energized structured water on bioenergetic function and oxidative stress in H9c2 cells

Sachithra S. Ranaweera [a], Juan P. Zuniga-Hertz [a,b], Ramamurthy Chitteti [a,b], Andrei V. Chernov [a,b], Hemal H. Patel [a,b,*]

[a] Department of Anesthesiology, University of California, San Diego, La Jolla, United States
[b] Veterans Affairs San Diego Healthcare System, La Jolla, United States

ARTICLE INFO

Keywords:
Energized structured water
Bioenergetics
Mitochondrial respiration
Cell viability
Oxidative stress
Gene expression analysis

ABSTRACT

The energized structured water (ESW) concept supposes water can be imbued with energetic frequencies or vibrations, improving its quality and providing various health benefits. While some studies claim benefits, the mechanisms and effects of ESW are not well understood. This study investigates the impact of ESW on cellular bioenergetic function and oxidative stress in H9c2 cells. H9c2 cells were pretreated with ESW or control water (CW) at equivalent dilutions. Mitochondrial function was assessed using the Agilent Seahorse XF Pro Analyzer. Cell viability and reactive oxygen species (ROS) production were evaluated under H_2O_2-induced oxidative stress conditions. Differential gene expression analysis and Gene Ontology (GO) enrichment were conducted to identify significantly affected genes and biological processes in ESW-treated H9c2 cells. Results demonstrated that ESW pretreatment significantly increased maximal and spare respiratory capacity in H9c2 cells. In addition, ESW treatment increased the glycolytic ATP production without affecting mitochondrial and total ATP production. ESW treatment enhanced cell viability and reduced ROS production in cells exposed to H_2O_2-induced oxidative stress. Based on differential gene expression analysis, 717 genes including *Myh1, Akr1b8, Hmox1, Kcng1, Ugt1a6, Clu, Gaa, Ftl1, Hspb7*, and Gba1 were up-regulated and 422 genes including *Hist1h2an, Slfn4, Rpl22l1, Polr2k, Il1rl1, Ndufb1, Atp5mkl1* were down-regulated by ESW compared to the controls. GO analysis indicated that ESW treatment significantly affects biological processes related to cellular stress response pathways. These findings suggest that ESW treatment may enhance cellular bioenergetics and stress resistance in H9c2 cells, potentially through modulation of gene expression related to stress responses and energy metabolism.

Introduction

Energized structured water (ESW) refers to liquid water that exhibits enhanced molecular organization compared to unstructured bulk water, characterized by the formation of coherent hydrogen-bonded networks and water clusters.[1–3] These clusters can range from small assemblies of a few molecules to larger, organized domains containing hundreds of water molecules, forming what are termed "coherent domains" or "exclusion zones (EZ) as shown in Fig. 1.[4] The molecular organization in ESW involves modified hydrogen bonding patterns, altered dipole orientations, and increased molecular ordering that extends beyond the typical random arrangement found in bulk water.[1,4–6] The structural modifications in ESW are associated with measurable changes in physical properties, including surface tension, viscosity, electrical conductivity, and optical characteristics, which may contribute to its distinct biological activities compared to conventional water.[1,4,6,7]

Emerging evidence suggests that water and biological systems possess remarkable quantum properties, typically observed at the microscopic level.[8,9] Although the precise mechanisms are still being investigated, some studies suggest that the organized molecular structure of structured water may enhance biological interactions by improving membrane permeability, altering ion transport, and modifying protein-water interactions.[10,11] Magnetic treatment alters water's physicochemical properties by converting kinetic energy of ions into electrical energy, making electrolyte ions more activated and easily absorbed by the body to promote biological activation of tissues and cells.[12] This process increases ionization and electrolyte mobility in magnetized water, which are considered critical factors for enhancing

* Corresponding author at: Department of Anesthesiology, University of California, San Diego, Biomedical Sciences Building, Mail Code 0629, 9500 Gilman Drive, La Jolla, CA 92093-0629.
E-mail address: hepatel@ucsd.edu (H.H. Patel).

https://doi.org/10.1016/j.explore.2025.103232
Received 10 May 2025; Received in revised form 26 June 2025; Accepted 31 July 2025
Available online 5 August 2025

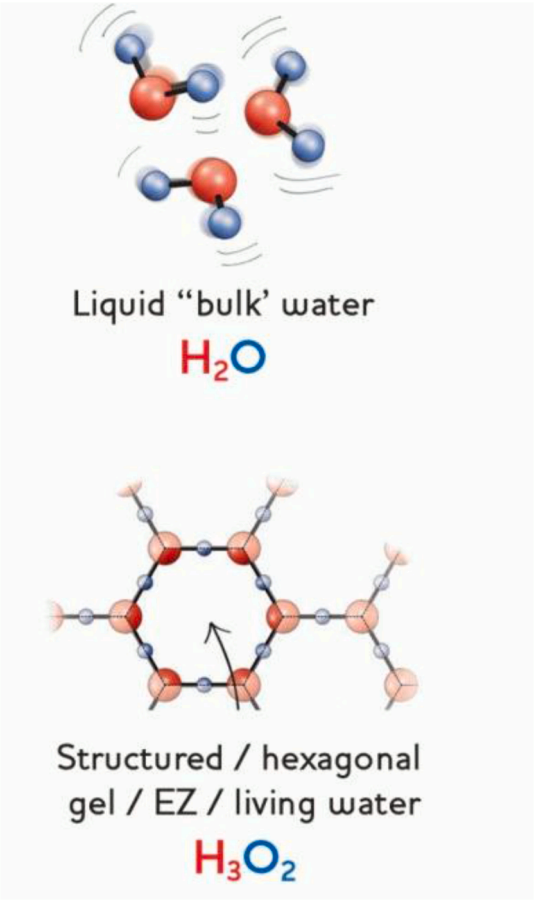

Fig. 1. Schematic representation of water molecular structures. The top panel illustrates conventional liquid "bulk" water (H_2O), characterized by randomly oriented water molecules. The bottom panel represents structured or "hexagonal" water (H_3O_2), also referred to as exclusion zone (EZ), gel, or living water, showing an ordered arrangement of water molecules forming a hexagonal lattice. Image source: Pollack, G. H. (2013). The fourth phase of water: Beyond solid, liquid, and vapor. Ebner & Sons.

enzyme activity and cellular functions.[12] In addition, magnetized water exhibits increased pH and electrical conductivity due to altered hydrogen bonding and ion hydration, which may enhance biological functions by improving ion transport, enzyme activity, and cellular signaling efficiency.[10–13]

The idea that water can have unique structural properties and potentially transfer information has gained attention and interest from researchers across various disciplines.[4,6,14,15] ESW is often associated with holistic health practices and alternative medicine. Previous investigations have documented diverse biological effects of structured water across multiple physiological systems and species.[4,16,17] Findings suggest that dairy cows that consumed magnetically treated water (MTW) have improved milk production and overall healthier conditions than those drinking untreated water.[18] Similarly, sheep exposed to MTW have demonstrated increased wool and meat production.[19] In addition, treatment of MTW improves Japanese quail's biochemical and physiological properties, which could help improve poultry productivity.[20] In metabolic health, structured water supplementation lowers blood glucose, glycated hemoglobin, and oxidative DNA damage in diabetic animal models.[21] Additionally, structured water increases cell viability and antioxidant activity in various cell culture systems.[22] Together, these findings highlight the biological relevance of structured water, demonstrating its potential to improve metabolic health and cellular function across diverse species and systems.

Based on the previous findings, it is possible that water can adopt a distinct state shown by an organized molecular structure, enabling it to retain and transfer energetic patterns or frequencies.[4,8] The ability of water to encode and transmit specific information could open new possibilities for personalized therapies, targeted drug delivery, and novel approaches to healthcare. While structured water demonstrates benefits in animal and human studies,[4,16] the cellular mechanisms underlying these effects, particularly on cardiac cell bioenergetics and gene expression, remain unexplored. Recent evidence suggests that topical magnetized saline water improves skin biophysical parameters,[23] while magnetized water activates autophagy and enhances photoprotection in keratinocytes,[24] supporting the therapeutic potential of water-based interventions in cellular applications.

Cardiac cells have exceptionally high energy demands and are particularly susceptible to mitochondrial dysfunction, which contributes to various cardiovascular pathologies including heart failure and ischemic heart disease[25] . However, it is unknown whether ESW improves mitochondrial respiratory capacity and oxidative stress resistance in cardiomyoblasts. The present study represents the first in vitro investigation to comprehensively assess ESW effects on bioenergetics function and transcriptomic responses in H9c2 cells, addressing a critical knowledge gap in understanding the cellular basis of structured water biological activity. H9c2 cells represent an ideal model for investigating ESW effects due to their high metabolic demands and dependence on mitochondrial function.[25] We hypothesize that ESW pretreatment increases respiratory capacity and reduces oxidative stress, inducing ROS levels in H9c2 cells compared to control water (CW), while modulating gene expression related to cellular stress response and energy metabolism. To test these hypotheses, we utilized Seahorse XF technology for bioenergetic analysis, ROS detection assays for oxidative stress assessment, and transcriptomic analysis to investigate the molecular mechanisms underlying ESW effects on H9c2 cells.

Materials and methods

Cell culture

H9c2 (CRL-1446™) cell line was purchased from the American Type Culture Collection (ATCC, Manassas, VA, USA). Cells were cultured in Dulbecco's Modified Eagle's Medium (DMEM) (GIBCO/BRL, 11,885,092) containing 5 mM glucose, supplemented with 10 % fetal bovine serum (FBS, Thermo Fisher Scientific, 16,000,044) and 1 % Penstrep (Penicillin/Streptomycin, GIBCO, 15,140,122). The cells were maintained in vented 75 cm^2 tissue culture flasks (Sarstedt, Germany) and incubated at 37 °C under 5 % CO_2. The cultures were routinely split, using trypsin (0.25 % Trypsin-EDTA, Gibco, 25,200–056) at 70–80 % confluency. Treatments of H9c2 were started at passages 5–8 in all experiments to preserve the characteristics of the cell lines.

Water imprinting method

ESW and CW samples were obtained from NES Health (Tampa, FL, USA), which specializes in producing imprinted water products. The ESW used in the current study was specifically formulated through NES Health's imprinting process, which was developed and perfected through multiple years of testing, to transfer energetic information aimed at enhancing cellular bioenergetics, antioxidant capacity, and stress response effects.[26] NES Health's imprinting process for the structured water samples was carried out using a proprietary fixed imprinter device equipped with the 940 nm infrared LED arrays (200 mW light flux), 400 nm UV LED arrays (30 mW light flux), red LED arrays (250 mw light flux), green LED arrays (250 mw light flux), 48 mA Bifilar coils (1 mT strength), and 8 kV electrostatic field generator. For the imprinting process, purified water (contains Himalayan sea salt 1 % or 0.29574 ml/oz, potassium chloride 1.5 % or 0.44361 ml/oz, magnesium chloride 1 % or 0.29574 ml/oz, potassium sorbate 0.2 % or 0.059148 ml/oz, citric acid 0.1 % or 0.02957 4 ml/oz) samples were

loaded onto the conveyor system of the imprinter device. As the water samples moved through the imprinter device, they were exposed to the illumination from the 940 nm infrared LED arrays, 400 nm UV LED arrays, red and green LED arrays, magnetic and electrostatic fields simultaneously for 10 s. After the exposure, the imprinted water samples were collected at the output of the imprinter device for further analysis and applications. A purified water sample was used as a CW without exposure to the imprinting process. ESW and CW samples were stored in amber-colored, sealed glass bottles at room temperature (15 °C-22 °C) in the dark to prevent potential degradation of imprinted properties and minimize environmental influences.

Structured water treatment

H9c2 cells were treated for 72 h. Cell culture media was refreshed daily, with the addition of either fresh media alone (control) or media containing ESW or CW at specific dilutions. The dilutions used were 1:10, 1:100, and 1:1000. This media replacement and treatment addition process was repeated daily throughout the 72-hour experimental period. The final volume added was 100 μL per well of treatment solution. These dilution ratios were selected based on preliminary studies conducted in our laboratory, which identified this concentration range as optimal for structured water biological effects on H9c2 cells. For the cellular functional assays (bioenergetics, viability, ROS), wells were assigned to treatment groups systematically across plates to ensure equal distribution of treatments within each experimental run. Technical replicates were distributed across multiple plates to account for plate-specific variability. The experimental design included three groups: 1) control cells cultured in normal growth medium alone, 2) cells treated with CW containing identical chemical composition but without energetic imprinting, and 3) cells treated with ESW that underwent complete electromagnetic imprinting process.

Bioenergetics assessment

Agilent Seahorse XF Pro Analyzer (Agilent Technologies, Santa Clara, California) was used to assess extracellular acidification rate (ECAR, mpH/min) and mitochondrial oxygen consumption rate (OCR, pmol/min) in H9c2 cells. Cells were plated at seeding densities 5 K, 10 K, 20 K, and 40 K to find the optimized cell seeding density, which was experimentally determined between 10 K and 20 K cells (Supplementary Figure 1A). This was followed by drug optimization tests, in which the optimal final well concentrations were experimentally determined to be 1.5 μM for oligomycin, 1.5 μM for carbonyl cyanide-p-trifluoromethoxyphenylhydrazone (FCCP), and 0.5 μM of rotenone and 0.5 μM of antimycin A (Rot/AA).

Mitochondrial stress tests were performed as suggested by the manufacturer (Agilent Seahorse XF Cell Mito Stress Test kit, 103,015–100) to determine non-mitochondrial respiration, basal respiration, proton-leak, ATP-linked respiration, mitochondrial maximal respiration, and spare respiratory capacity. Briefly, H9c2 cells were seeded in an XF 96-well plate at 1×10^4 cells/well density. Afterward, the cells were exposed to ESW and CW at dilutions of 10^{-1}, 10^{-2}, and 10^{-3} in normal growth media for 72 h.[27] Control cells were treated solely with normal growth media. Fresh samples were prepared daily throughout the treatment, and the cell culture media were replaced accordingly. On the day of the assay, the cell culture media were substituted with Agilent XF DMEM base medium supplemented with 1 mM pyruvate, 2 mM glutamine, and 10 mM glucose. Subsequently, the cells were incubated for 1 hour in a CO_2-free environment at 37 °C to eliminate CO_2 and prevent pH disturbances. The mitochondrial stress assay was performed with the sequential addition of oligomycin (1.5 μM), FCCP (1.5 μM), and a mixture of Rot/AA (0.5 μM). The non-mitochondrial oxygen consumption rate is the minimum OCR measured after the Rot/AA injection. Basal respiration differs between the OCR before applying the first agent and the non-mitochondrial oxygen consumption rate. Maximal respiration is the difference between the OCR amplitude observed in the presence of FCCP and the non-mitochondrial oxygen consumption rate. The spare respiratory capacity is the difference between maximal and basal respiration (Supplementary Figure 1B). All data were normalized to the basal level of the respiration rate (OCR just before the application of any agent, 100 %).

To quantify the overall cellular ATP production rate and distinguish the respective contributions of glycolysis and mitochondrial respiration, we employed the XF Real-Time ATP Rate Assays, utilizing 1.5 μM oligomycin and 0.5 μM of ROT/AA. The results were normalized to the number of cells quantified by Hoechst staining using Cytation 5 (Agilent Technologies, Santa Clara, California) and images in software (Gen5). Results were analyzed by Wave Desktop Software 2.6 (Agilent Technologies, Santa Clara, California) and using Seahorse analytics by Agilent Technologies (https://www.agilent.com/en/product/cell-analysis/real-time-cell-metabolic-analysis/xf-software/agilent-seahorse-analytics-787485).

Cell viability assay

Cell viability was examined using the XTT assay (Thermo Fisher Scientific, Waltham, Massachusetts). H9c2 cells were plated in a 96-well plate at 1×10^4 cells/well. After adhering overnight, H9c2 cells were incubated with ESW and CW, at dilutions of 10^{-2}, and 10^{-3}, in normal growth media for 72 h, except for the control group receiving the medium instead. Oxidative stress was induced by administering 125 μM H_2O_2 and 250 μM H_2O_2. H9c2 cells were exposed to H_2O_2 (125 μM and 250 μM) in DMEM without FBS at 37 °C in a humidified atmosphere containing 5 % CO_2 for 1 hour. After that, cells were incubated with XTT at 37 °C for another 4 h. Absorbance was examined with a microplate reader at a wavelength of 450 nm and 660 nm.

Reactive oxygen species analysis

To assess the impact of ESW on cellular oxidative stress induced by ROS, H9c2 cells were cultured in cellvis-P96 glass-bottom 96-well plates at a density of 1×10^4 cells per well. Cells were treated with ESW or CW at dilutions of 10^{-2} and 10^{-3} in normal growth media for 72 h, with the control group receiving only medium. Subsequently, cells were exposed to 250 μM H_2O_2 for 1 hour. Intracellular ROS levels were quantified using the DCFDA/H2DCFDA cellular ROS assay kit (Abcam, ab 113,851). Treated cells were washed with 1X buffer after medium removal and incubated with 7 μM DCFH-DA in PBS at 37 °C for 45 min. Following two washes to remove excess dye, fluorescence readings were measured with excitation at 485 nm and emission at 535 nm by Cytation 5 (Agilent Technologies, Santa Clara, California) fluorescent plate reader. The percentage increase in intracellular ROS was calculated based on the fluorescence intensity of DCF in each treatment group relative to the control. The images of H9c2 cells were also acquired with a Keyence microscope under blue and green fluorescent filters.

RNA isolation, library preparation, sequencing and data analysis

Total RNA was extracted using a RNeasy Plus Mini Kit (Qiagen) following ESW and CW treatment at dilutions of 10^{-2} for 72 h. RNA concentrations and quality were determined using NanoDrop absorbance ratios at 260/280 nm and 260/230 nm. RNA integrity was determined using the Agilent Bioanalyzer Nano RNA chip. RNA (500 ng, 3 replicates/group) with RIN $\geq$ 8.0 was used for RNA-seq. High-throughput sequencing was conducted at the IGM Genomics Center (UCSD, La Jolla, CA, USA) on Illumina NovaSeq X Plus. RNA-seq data (58.8–107 million reads/sample) were saved in FASTQ format. For RNA-seq analysis, samples were randomly assigned identification codes and processed randomly to minimize batch effects and processing bias. RNA extraction, library preparation, and sequencing were conducted with samples identified only by randomized codes, with treatment identities

revealed only after initial bioinformatic analysis.

All steps of data processing and downstream analysis were conducted at the Texas Advanced Computing Center (TACC) The University of Texas at Austin. Software used for RNA-seq analyses is summarized in Bioinformatics Resources (Supplementary Table 1). FASTQ files were pre-filtered to remove low-quality bases, TruSeq dual-index adapter sequences, and unpaired reads using Fastp utility.[28] Transcript-level mapping was conducted in Salmon aligner[29] using rat (*Rattus norvegicus*) reference genome and transcriptome assembly version GRCr8 (GCF_036323735.1). The quality of RNA-seq, mapping, and quantification were assessed using the MultiQC tool.[30] All samples had high-quality scores.

Gene-level quantification and annotation were done using Tximeta utility.[31] Gene count matrices were normalized, and differential expression analyses were done in DESeq2[32] using a generalized linear model in which counts for each gene and sample were modeled using a negative binomial distribution with fitted means and gene-specific dispersions.[32] Outlier samples were detected by Cook's distance method and excluded. The adjusted (shrunken) $\log_2$FC values were calculated using the ashr method.[33] Significant DEGs defined by Wald test $P < 0.05$ and $P_{adj} < 0.1$ (or both) and used in downstream analyses. $\log_2$FC estimates were shrunken towards the prior using the ashr method.[33] Batch effects were controlled using removeBatchEffect[34] and RUVseq[35] functions. DEGs were visualized using PCAtools, and EnhancedVolcano Bioconductor packages.

Enrichment analyses of protein-coding and non-coding RNA (ncRNAs) DEGs annotated in the GO database and fitting the standard statistical criteria ($P_{adj} < 0.1$) were conducted to estimate significant GO biological processes, cellular components and molecular functions in comparison groups. The arbitrary *post hoc* filtering of DEGs by $\log_2$FC > 0.2 or log2FC < -0.2 was applied to predict up- or down-regulated GO terms, respectively. Biological interpretations of signaling pathways and GO terms were conducted using default parameters in clusterProfiler[36] based on significance scores (q-values < 0.05) calculated by Fisher exact test[36] and adjusted using Benjamini-Hochberg procedure. KEGG[37] and GO public databases[38] were used for data mining. Data were analyzed and visualized in Bioconductor,[39] R-studio (version 2023.06.1) and Cytoscape (version 3.10.2).[40,41]

Statistical analysis

Statistical analyses were performed using GraphPad Prism Version 10.2.2, which was also used to generate all graphs. A one-way analysis of variance (ANOVA) test, followed by Tukey's multiple comparisons test, was used to compare multiple groups to assess statistical significance. Unpaired Student's T-tests were used for two-group comparisons. All results are expressed as mean ± standard error of the mean (SEM). A p-value < 0.05 was considered to indicate a statistically significant difference.

Results

Effects of ESW on mitochondrial respiration in H9c2 cells

We performed the XF Cell Mito Stress assay to investigate the impact of the ESW on oxidative phosphorylation (OXPHOS) in H9c2 cells. The Mito Stress assay results revealed that treating H9c2 cells with ESW significantly enhanced mitochondrial maximal respiration and spare respiratory capacity at dilutions of 10^{-2} and 10^{-3} (Fig. 2B and 2C). However, no significant difference was observed at the 10^{-1} dilution compared to the controls (Fig. 2A). After injecting the uncoupling agent FCCP, the OCRs showed that ESW-treated cells exhibited the highest maximal respiration (OCR %) at the 10^{-2} dilution (209 ± 6) and the 10^{-3} dilution (202 ± 5) compared to maximal respiration of the control group (180 ± 5) and the cells treated with CW at the same dilutions (10^{-2}: 187 ± 5 and 10^{-3}: 185 ± 5). Furthermore, the spare respiratory capacity was augmented in ESW-treated cells at both the 10^{-2} dilution (135 ± 6) and the 10^{-3} dilution (128 ± 5) compared to the spare respiratory of the control group (106 ± 5) and the cells treated with CW at the same dilutions (10^{-2}: 115 ± 5 and 10^{-3}: 116 ± 6). No significant differences between the groups were observed in non-mitochondrial respiration, basal respiration, proton-leak, and ATP-linked respiration. These results suggest that ESW treatment at specific dilutions (10^{-2} and 10^{-3}) enhances mitochondrial bioenergetics in H9c2 cells by increasing their maximum and spare respiratory capacity.

Effects of ESW treatment on ATP production in H9c2 cells

The total cellular ATP production rate and fractional contributions from glycolysis and oxidative phosphorylation were analyzed simultaneously using the ATP rate assay. The ATP rate assay results indicate that treatment with ESW leads to a significant increase in glycolytic ATP production in H9c2 cells at the 10^{-2} dilution (5.4 ± 0.3 pmol/min/1000 cells) and 10^{-3} dilution (5.7 ± 0.2 pmol/min/1000 cells) when compared to both control group (4.4 ± 0.1 pmol/min/1000 cells) and cells treated with CW at the same dilutions 10^{-2} (4.6 ± 0.3 pmol/min/1000 cells), and 10^{-3} (4.8 ± 0.2 pmol/min/1000 cells) (Fig. 3). However, no significant changes were observed in either mitochondrial or total ATP production rate in ESW or CW-treated groups compared to the control group. This suggests that the ESW treatment enhances the glycolytic pathway without involving mitochondrial ATP production.

The protective effects of ESW on H_2O_2-induced cytotoxicity

Cell viability was determined to assess the effects of the ESW on H_2O_2-induced cytotoxicity in H9c2 cells. Treatment with ESW or CW for 72 h did not affect the viability of H9c2 cells under physiological conditions compared to the non-treated control group. This indicates that the treatments alone did not exert cytotoxic effects on the cells. Exposure of H9c2 cells to 125 μM H_2O_2 and 250 μM H_2O_2 led to a significant decrease in cell viability, reducing it to 60 ± 3 % and 32 ± 1 %, respectively, compared to the viability of the H_2O_2-untreated control group, which was set at 100 % (Fig. 4).

Exposing cells to 125 μM and 250 μM of H_2O_2 followed by ESW at a 10^{-2} dilution pretreatment, attenuated H_2O_2-induced reduction in cell viability to 86 ± 2 % and 43 ± 1 %, respectively. This improvement was significant compared to the cell viability of the model group (60 ± 3 % and 32 ± 1 %) and to that of cells treated with CW at the same 10^{-2} dilution (73 ± 3 % and 38 ± 1 %) (Fig. 4A). Similarly, pretreatment with ESW at a 10^{-3} dilution also significantly improved cell viability to 83 ± 3 % and 42 ± 2 % in the presence of 125 μM and 250 μM H_2O_2, respectively. These values were significantly higher compared to the model group treated with H_2O_2 alone and the cells pretreated with CW at the same 10^{-3} dilution, which showed cell viabilities of 70 ± 2 % and 34 ± 1 %, respectively (Fig. 4B). In addition, the morphologies of H9c2 cells treated with H_2O_2 in the presence of ESW or CW were observed with an inverted phase-contrast microscope. Control H9c2 cells were normal with long fusiform shapes. H_2O_2 treatment induced distinctive morphological changes, including cell shrinkage, irregular shapes, and widened intercellular gaps, suggesting cellular damage. However, the proportion of abnormal cells was ameliorated in ESW-treated cells compared to the control groups (Fig. 4C). These results suggest that ESW reduces oxidative stress-induced cytotoxicity in H9c2 cells.

Effects of ESW on intracellular ROS production

When cells encounter H_2O_2, they undergo oxidative stress, resulting in a rise in intracellular ROS levels. To evaluate whether the ESW influences H_2O_2-induced ROS generation, intracellular ROS levels were measured using the DCFH-DA method. When H9c2 cells were exposed to H_2O_2, pretreatment with ESW at a 10^{-2} dilution significantly reduced ROS production by 37 % of the control level, set at 100 %. In

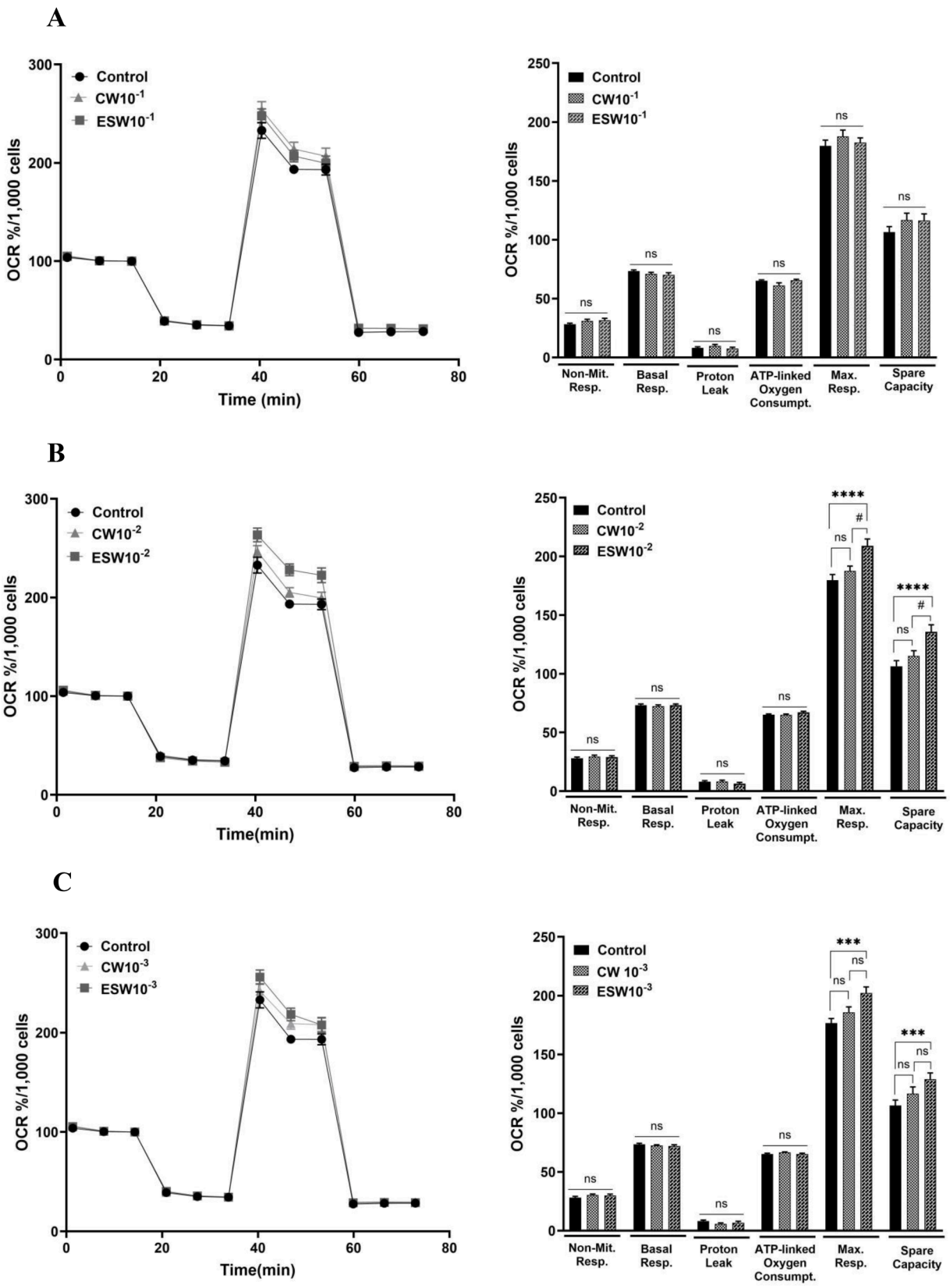

Fig. 2. Bioenergetic profile of H9c2 cells treated with ESW and CW for 72 h. OCR was analyzed after injection of respiratory chain inhibitors at specified time points. **A.** Mitochondrial stress oxygen consumption rate curve and mitochondrial parameters in cells treated with ESW and CW at the dilution of 10^{-1}. **B.** Mitochondrial stress oxygen consumption rate curve and mitochondrial parameters in cells treated with ESW and CW at the dilution of 10^{-2}. **C.** Mitochondrial stress oxygen consumption rate curve and mitochondrial parameters in cells treated with ESW and CW at the dilution of 10^{-3}. Data are expressed as mean ± SEM ($n = 5$), $\#P < 0.05$ versus the CW group, and $*p < 0.05$ versus the control group.

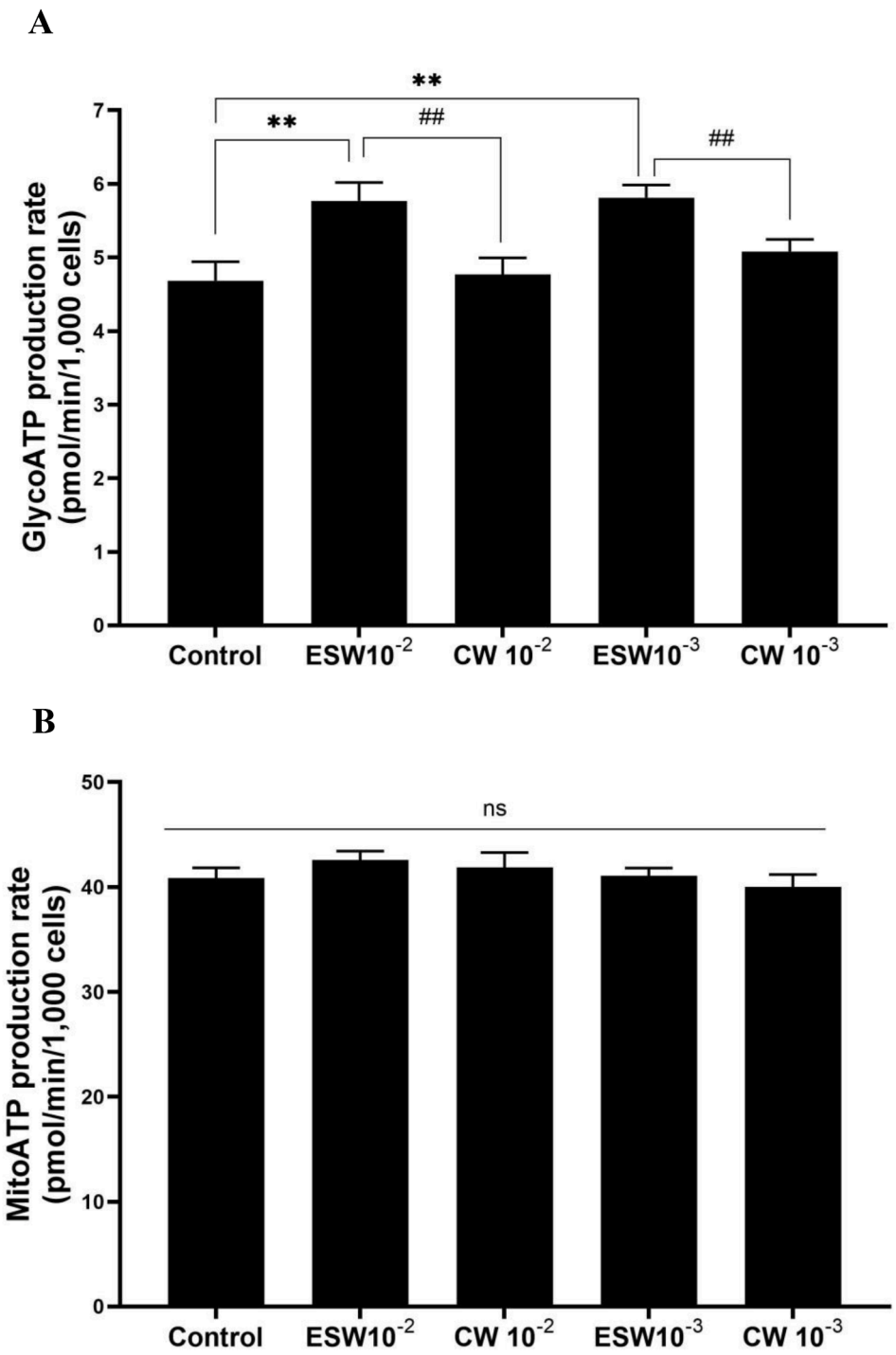

Fig. 3. Quantification of ATP production rate. Seahorse XF Real-Time ATP Rate Assays were performed in H9c2 cells under treatment of ESW or CW. **A**. Glycolytic ATP production rate and **B**. Mitochondrial ATP production rate is shown. Data are expressed as mean ± SEM ($n = 5$). #$P < 0.05$ versus the CW group and *$p < 0.05$ versus control group.

comparison, pretreatment with control water (CW) at the same 10^{-2} dilution reduced ROS production by 24 % of the control level. Similarly, pretreatment with ESW at a 10^{-3} dilution reduced ROS levels by 34 % compared to the control level. In addition, CW pretreatment at the same 10^{-3} dilution reduced ROS levels by 17 % of the control level (Fig. 5). These results suggest that ESW pretreatment significantly reduced ROS production compared to both the control and the CW pretreatment groups.

Effects of ESW on differential gene expressions in H9c2 cells

Transcriptome analysis was conducted to observe the effect of ESW and CW on the expression levels of genes in H9c2 cells. Principal component (PC) analysis applied to the RLOG-converted count matrix determined that ESW, CW and control groups exhibited distinct clustering with low sample-to-sample variability (Fig. 6A). As shown in Fig. 6B, ESW resulted in 717 genes up-regulated ($P_{adj} < 0.1$, $\log_2FC > 0.2$) and 419 genes down-regulated ($P_{adj} < 0.1$, $\log_2FC < -0.2$) compared to the control group, whereas the numbers of up- /down-

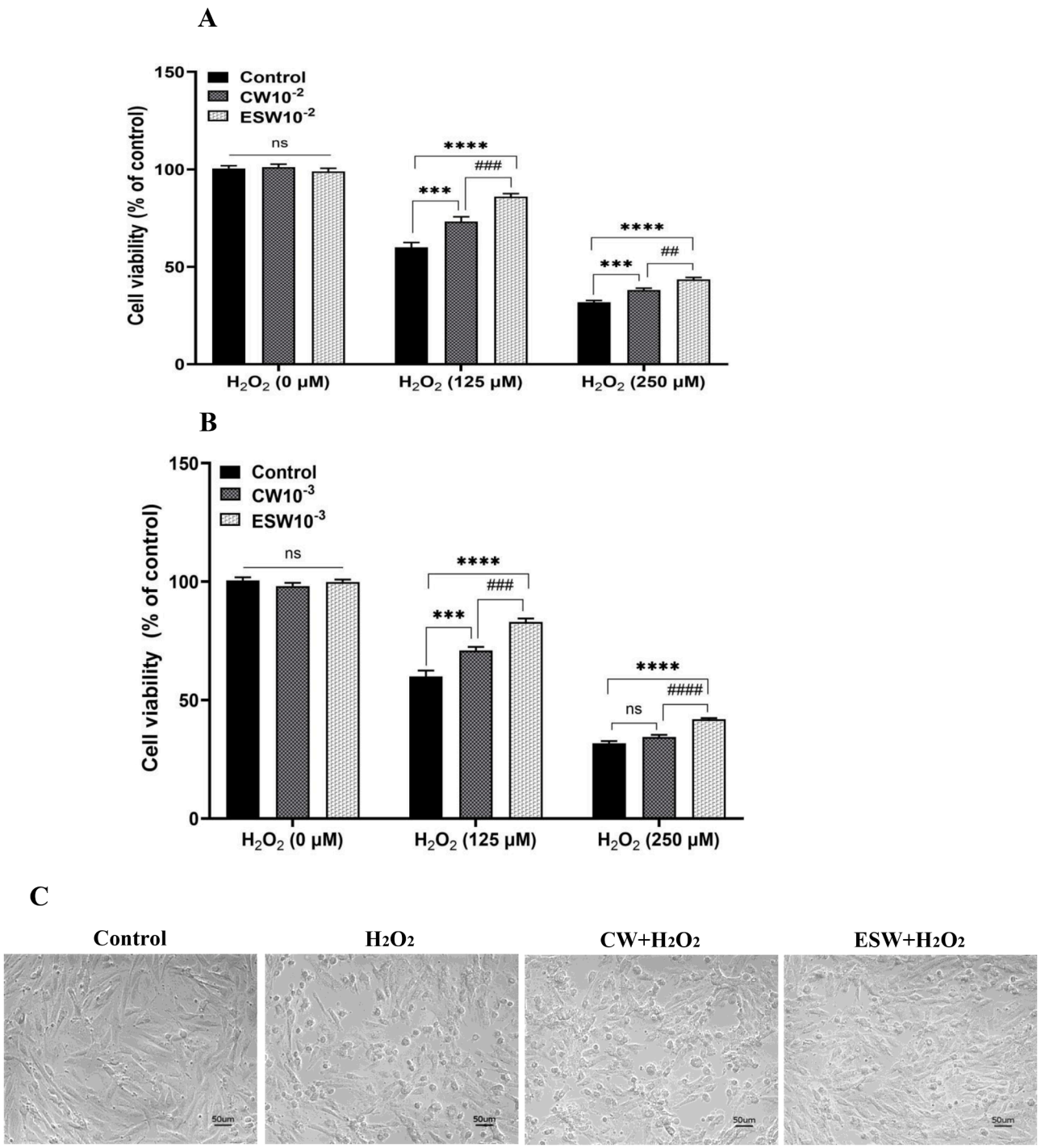

Fig. 4. Effect of ESW on cell viability of H9c2 cardiomyocytes subjected to H_2O_2-induced oxidative damage. **A.** Cell viability at the dilution 10^{-2}, **B.** Cell viability at the dilution 10^{-3}, **C.** Morphological changes in H9c2 cells were preincubated CW and ESW at the dilution 10^{-2} for 72 h and then treated with 250 μM H_2O_2 for 1 h. Cell morphology was examined under an inversion microscope. Scale bar: 50 μm. Data are expressed as mean ± SEM ($n = 5$). #$P < 0.05$ versus the CW group and *$p < 0.05$ versus model group (Control group).

regulated genes ($P_{adj} < 0.1$) in ESW treated group compared with CW treated group were 859 and 672, respectively. In contrast, the CW-treated group showed only 9 significantly up-regulated and 11 significantly down-regulated genes when compared to the control group. Significant up- and down-regulated protein-coding, annotated genes are presented on volcano scatter plots for all comparison groups (Fig. 6C, Table 1). Top upregulated genes in ESW-treated H9c2 cells included *Myh1, Akr1b8, Hmox1, Kcng1, Ugt1a6, Clu, Gaa, Ftl1, Hspb7*, and *Gba1*. Top downregulated genes included *Hist1h2an, Slfn4, Rpl22l1, Polr2k, Il1rl1, Ndufb1, and Atp5mkl1*, compared to both control and CW groups.

Gene ontology (GO) analysis

GO analysis revealed (Fig. 7) that ESW significantly increased biological process related to extracellular matrix organization, extracellular structure organization, external encapsulating structure organization, response to mechanical stimulus, response to hydrogen peroxide, cellular response to reactive oxygen species, glucose metabolic process,

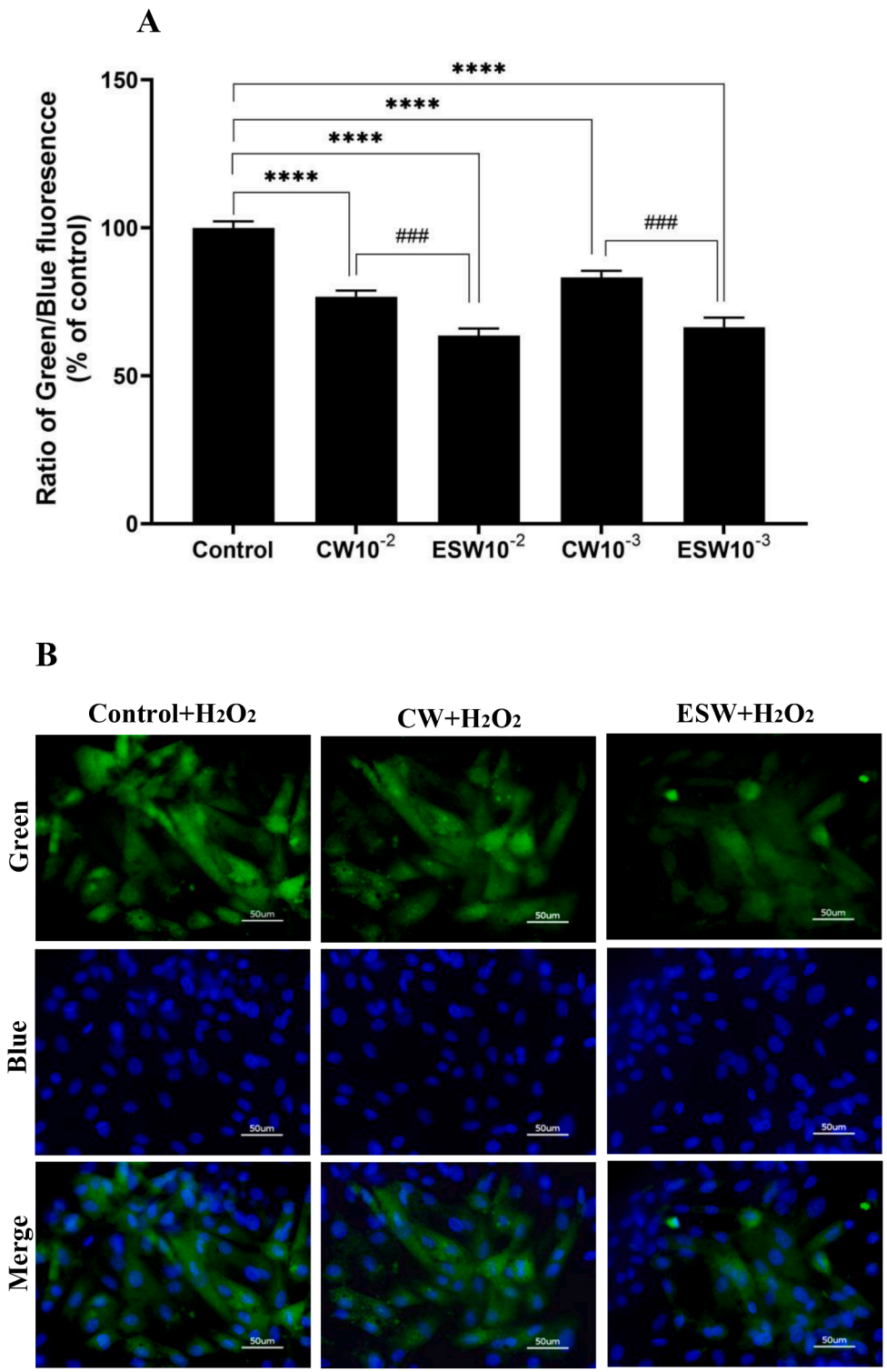

Fig. 5. Effect of ESW on ROS production of H9c2 cardiomyocytes subjected to H_2O_2-induced oxidative damage. H9c2 cells were preincubated CW and ESW at the dilutions 10^{-2} and 10^{-3} for 72 h and then treated with 250 μM H_2O_2 for 1 hour. **A**. relative absorbance of Green/Blue fluorescent to control group. Data are expressed as mean ± SEM ($n = 5$). #$P < 0.05$ versus the CW group and *$P < 0.05$ versus the model group (Control). **B**. Green (ROS staining), blue (DAPI nuclear staining), and merge images of cells treated with ESW and CW at the dilution 10^{-2}. Scale bar: 50 μm.

positive regulation of reactive oxygen species metabolic process, regulation of reactive oxygen species metabolic process, cellular response to oxidative stress, cellular response to chemical stress, glucose 6−phosphate metabolic process, regulation of cellular response to stress, compared with both control and CW treated groups. In contrast, the CW-treated group showed no significant changes in these biological processes compared to the control group.

Discussion

The present study investigated the effects of ESW on mitochondrial respiration, ATP synthesis, and oxidative stress-induced cytotoxicity in

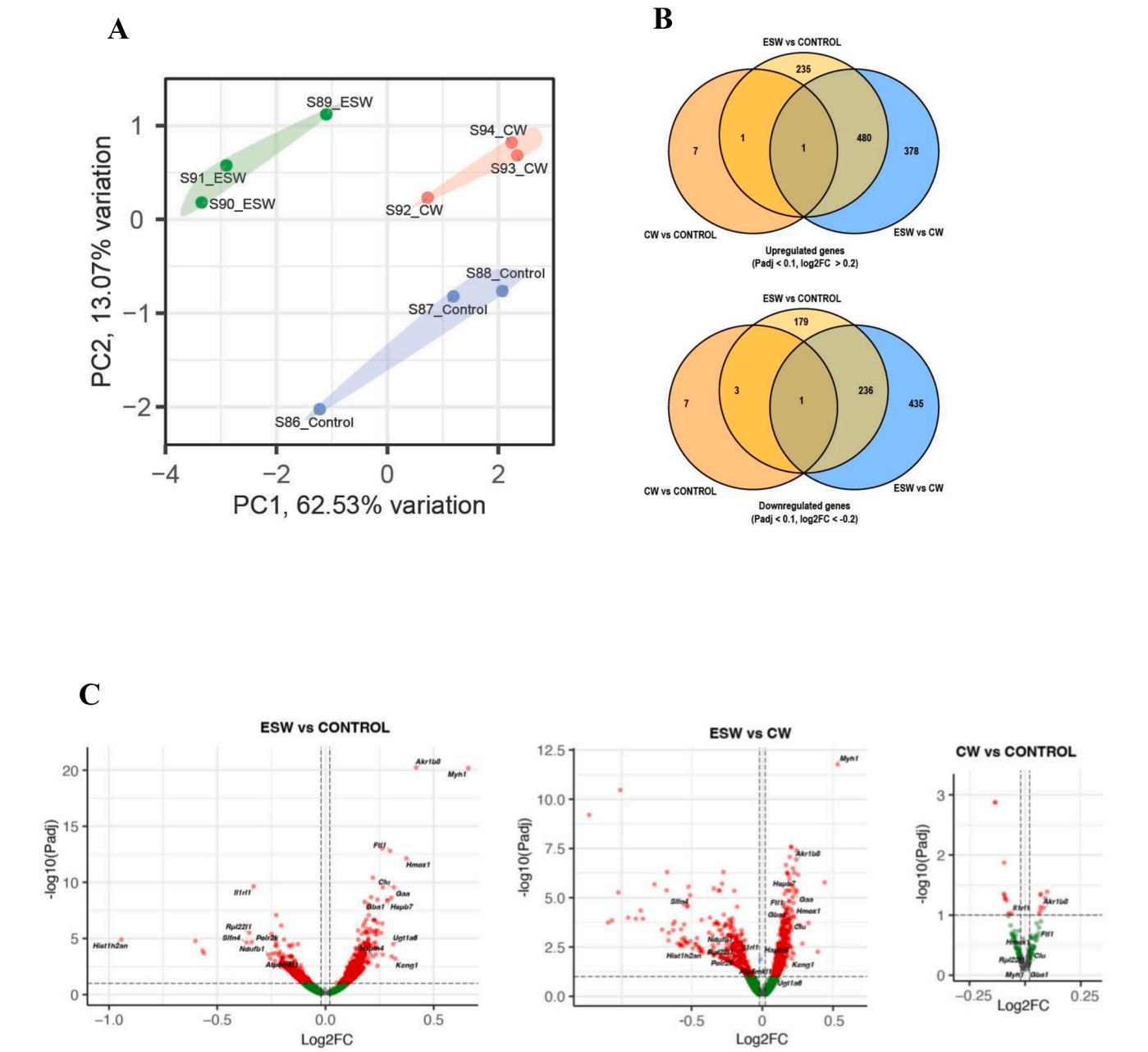

Fig. 6. Effects of ESW on differential gene expression in H9c2 cells. **A.** Principal component analysis of normalized gene counts. Colored areas indicate cluster overlaps according to respective legends (Green color: ESW samples S89 through S91. Red color: CW samples S92 through S94. Blue color: Control samples S86 through S88). **B.** Venn diagram of the analyzed up- and down-regulated DEGs in each group (ESW vs control, ESW vs CW, and CW vs control). **C.** Volcano scatter plots (-log10 Padj vs log2FC) of significant DEGs in ESW vs Control, ESW vs CW, CW vs Control. Red and blue colors indicate significant up- and down-regulated DEGs, respectively above (red) or below (blue) the log2FC threshold. Gray dots - genes below significance and FC thresholds. Thresholds (log2FC > 0.2 or log2FC < -0.2) and -log10Padj < 0.1 are indicated by dashed lines. Selected top up-and down-regulated DEGs are labeled. The list of top DEGs is included in Table 1. Experiments that were performed in triplicate ($n = 3$) for each experimental group.

H9c2 cells. Our results demonstrated that pretreatment with ESW significantly increased both mitochondrial maximum respiration and spare respiratory capacity in H9c2 cells. Additionally, our findings indicated that ESW enhanced glycolytic ATP production without affecting mitochondrial and total ATP production. Furthermore, ESW treatment reduced oxidative stress-induced cytotoxicity and decreased ROS production in H9c2 cells. RNA-seq analysis reveals that ESW exerts a protective effect by modulating the expression of genes related to cellular stress response and energy metabolism in H9c2 cells.

The present study investigated the effects of ESW on mitochondrial respiration, addressing the critical knowledge gap regarding ESW's impact on cellular bioenergetic function. Our results demonstrated that ESW significantly enhanced both maximal respiration and spare respiratory capacity in H9c2 cells, directly supporting our hypothesis and providing direct evidence for ESW's bioenergetic effects. The mitochondrial stress assay evaluates key parameters of mitochondrial function and respiratory capacity in living cells.[42] Maximal respiration is the maximum rate of oxygen consumption that cells can achieve when mitochondrial function is uncoupled.[43] Mitochondrial spare respiratory capacity refers to the ability of mitochondria to respond to increased energy demands or stress by boosting their respiratory activity beyond the baseline requirements.[44] It represents the reserve capacity available

Table 1
Top up- and down-regulated genes in ESW treated group when compared to both control and CW treated group.

Symbol	Gene name	log2FC (ESW vs Control)	log2FC (ESW vs CW)	Padj-value (ESW vs Control)	Padj-value (ESW vs CW)
Myh1	myosin heavy chain 1	0.66	0.54	4.17E-21	7.94E-13
Akr1b8	aldo-keto reductase family 1, member B8	0.42	0.24	6.50E-21	1.71E-07
Hmox1	heme oxygenase 1	0.38	0.21	8.01E-13	5.12E-05
Kcng1	potassium voltage-gated channel modifier subfamily G member 1	0.36	0.22	4.52E-04	9.76E-03
Ugt1a6	UDP glucuronosyltransferase family 1 member A6	0.33	0.11	2.37E-05	9.38E-02
Clu	clusterin	0.32	0.19	3.36E-10	1.56E-04
Gaa	alpha glucosidase	0.31	0.23	2.30E-09	5.45E-06
Ftl1	ferritin light chain 1	0.30	0.18	3.60E-13	4.29E-05
Hspb7	heat shock protein family B (small) member 7	0.29	0.23	5.24E-09	4.19E-06
Gba1	glucosylceramidase beta 1	0.29	0.20	5.27E-09	9.48E-05
Hapln4	hyaluronan and proteoglycan link protein 4	0.27	0.18	2.48E-04	8.03E-03
Hist1h2an	histone cluster 1, H2an	−0.92	−0.50	7.38E-06	3.18E-03
Slfn4	schlafen family member 4	−0.39	−0.52	1.67E-05	5.38E-06
Rpl22l1	ribosomal protein L22 like 1	−0.37	−0.18	2.19E-06	6.24E-03
Polr2k	RNA polymerase II, I and III subunit K	−0.36	−0.18	1.60E-05	9.23E-03
Il1rl1	interleukin 1 receptor-like 1	−0.33	−0.15	2.80E-10	6.63E-03
Ndufb1	NADH:ubiquinone oxidoreductase subunit B1	−0.28	−0.23	2.03E-04	2.18E-03
Atp5mkl1	ATP synthase membrane subunit K like 1	−0.27	−0.16	4.50E-04	1.98E-02

ESW: Energized structured water, CW: Control water, log2FC: Log2 fold changes, Padj-value: Benjamini-Hochberg adjusted p-value.

for cells to meet sudden energy demands or cope with cellular stressors.[44,45] The increase in these parameters signifies an improvement in mitochondrial function and cellular bioenergetic capacity.[45] Cells with enhanced mitochondrial maximum respiration and spare respiratory capacity are better equipped to produce energy efficiently and respond effectively to physiological and environmental challenges.[44–46] The depletion of spare respiratory capacity has been associated with various pathologies in tissues with high energy requirements, including the heart.[44,45] The present study revealed that the ESW treatment at specific dilutions (10^{-2} and 10^{-3}) enhanced mitochondrial bioenergetics in H9c2 cells by increasing their maximum and spare respiratory capacity. These improvements in mitochondrial function by treatment of ESW can potentially confer cytoprotective effects, enhance energy metabolism, and improve the cell's ability to cope with metabolic stresses, ultimately supporting its survival and function. The findings are consistent with previous studies showing that diabetic rats consuming magnetized water exhibited reduced weight gain despite similar food intake,[21] suggesting an increased metabolic rate. The increased spare respiratory capacity may provide a cellular mechanism for this enhanced metabolic activity, as improved mitochondrial bioenergetic reserves enable more efficient energy utilization and increased basal metabolic rates.

The present study demonstrated that pretreatment of ESW increased glycolytic ATP production without changing the mitochondrial ATP production in H9c2 cells compared to the control groups. The increase in glycolytic ATP production indicates that ESW treatment stimulated the glycolysis pathway in H9c2 cells. This could imply the treatment's specific modulation of cellular energy metabolism, potentially through alterations in glycolytic enzyme activity or glucose uptake.[47] Glycolysis typically contributes a small amount of ATP compared to mitochondrial oxidative phosphorylation in cardiac cells.[48] Therefore, even a significant increase in glycolytic ATP by treatment of ESW may not substantially impact the overall cellular ATP levels. Glycolysis can generate ATP more quickly than oxidative phosphorylation in mitochondria. Increasing glycolytic ATP production allows cells to meet immediate energy demands, such as during periods of high activity or stress.[49] Cells gain metabolic flexibility by enhancing glycolysis without impacting mitochondrial ATP production.[50] Therefore, increasing glycolytic ATP production can be advantageous in environments with limited oxygen availability or during hypoxic conditions, ensuring continued ATP production to support cellular functions.[47] It is important to note that while the ESW treatment selectively enhanced glycolytic ATP production, it did not impair mitochondrial function, as evidenced by the unchanged mitochondrial and total ATP levels. This is consistent with the unchanged ATP-linked OCR observed in the mitochondrial stress assay, which represents the amount of oxygen consumption dedicated to ATP production, as measured by the decrease in OCR after oligomycin injection. Together, these results suggest that ESW increases the cells' potential for energy production under stress conditions without affecting basal mitochondrial ATP output. Therefore, enhanced glycolytic ATP production in H9c2 cells by ESW may support cardiac cell survival, energy demands, and metabolic adaptations, particularly during ischemia, hypoxia, and pathological cardiac remodeling.[47,48,51]

Enhanced mitochondrial bioenergetics in ESW-treated H9c2 cells may be attributed to the structured water's quantum properties. Structured water forms EZ around proteins and membranes, enhancing energy storage and quantum energy transfer.[52] Approximately 3 % of intracellular water exhibits non-bulk properties, facilitating quantum energy transfer via structured layers around proteins.[53] At mitochondrial membranes, water interfaces capture energy and convert it into coherent electromagnetic signals that boost electron transport chain efficiency.[54] Meta-analysis reveals precise quantum entanglement in water assemblies,[55] suggesting ESW optimizes these quantum structures around mitochondrial proteins to improve maximal respiration and spare respiratory capacity.

Oxidative stress caused by ROS is considered a critical factor in the pathological development of myocardial infarction.[56] Exposure to H_2O_2 has been shown to elevate intracellular ROS levels, leading to antioxidant depletion, mitochondrial dysfunction, increased lipid peroxidation, and apoptosis in H9c2 cells.[57–61] As expected, the results demonstrate that H_2O_2 treatment induced dose-dependent cytotoxicity in H9c2 cells due to the oxidative stress caused by ROS. The subsequent experiments aimed to determine if pretreatment with ESW or CW could protect the cells from this H_2O_2-induced cytotoxicity. Both groups demonstrated an increase in cell viability and a decrease in ROS production. However, the protective effects of ESW were more pronounced than those observed with CW treatment at the same dilutions (Fig. 5). A previous study has reported that structured water demonstrated several biological effects, including increased cell viability and cytokine expression in normal cells and suppressed viability in MCF-7 cancer cells.[22] These enhanced cellular bioactivities have been strongly associated with the antioxidant properties of structured water. Such experimental findings suggest that water, depending on its structure, may play a crucial role in cellular bioactivities, primarily through its antioxidant effects.[22]

RNA-seq analysis revealed that ESW modulates the genes related to stress response and energy metabolism in H9c2 cells. Genes related to energy metabolism demonstrated significant upregulation, with *Myh1*

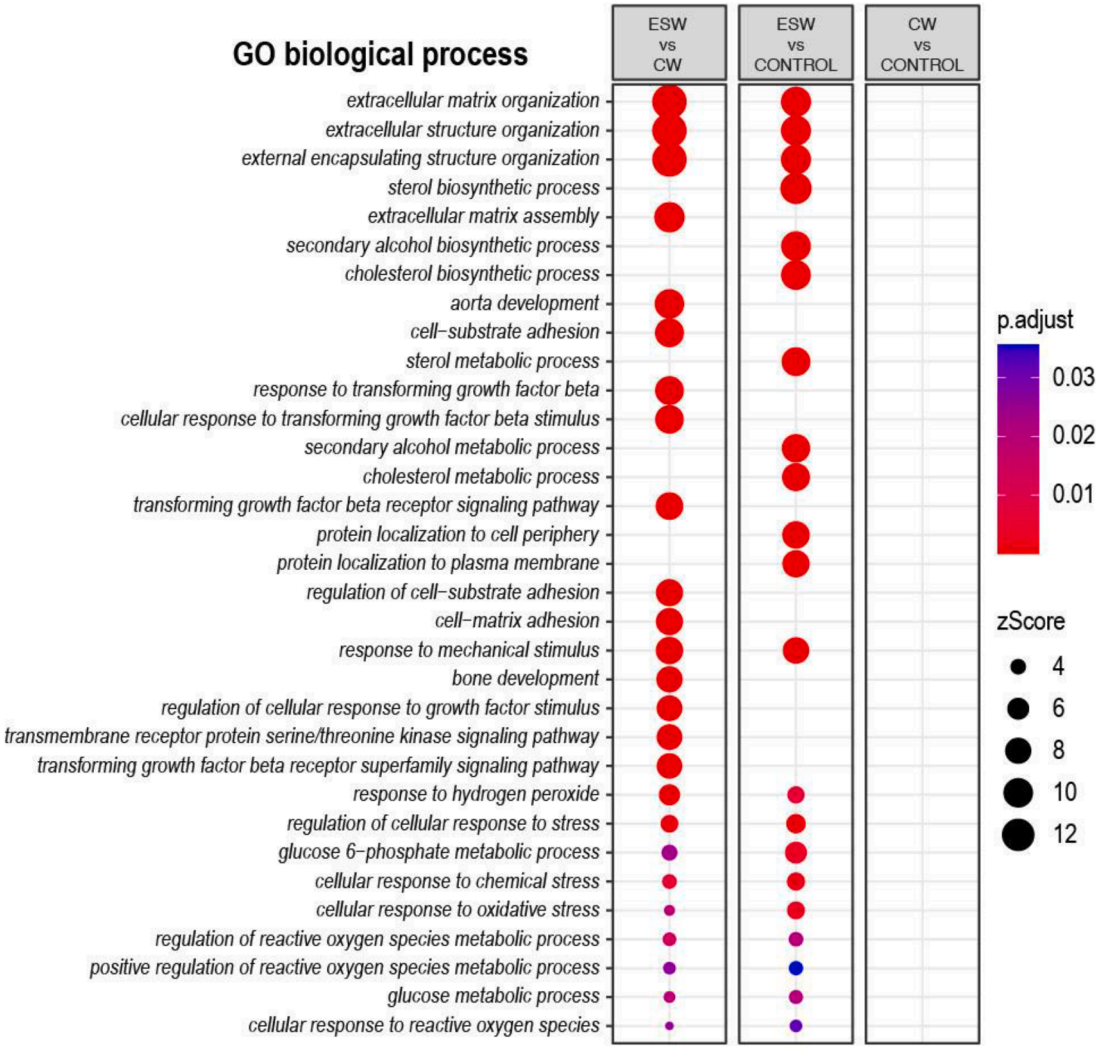

Fig. 7. Gene Ontology (GO) biological processes were identified by enrichment analysis of significant DEGs ($P_{adj} < 0.1$). Circle size corresponds to z-scores, colors indicate P_{adj} ($P_{adj} < 0.1$, blue to red colors – lower to higher significance) according to the scales.

gene encoding a key myosin heavy chain protein that plays a crucial role in ATP hydrolysis,[62] and *Gaa* playing a key role in providing glucose for energy production through glycolysis by catalyzing the hydrolysis of α−1,4 and α−1,6-glucosidic bonds of glycogen in lysosomes.[63] Antioxidant and detoxification genes showed enhanced expression, including *Akr1b8, Hmox1*, and *Ugt1a6. Akr1b8* reduces cytotoxic α, β-unsaturated carbonyls to less toxic alcohol forms in a NADPH-dependent manner.[64] *Hmox1* protects cells by breaking down heme into biliverdin, carbon monoxide, and iron. Biliverdin becomes bilirubin, an antioxidant.[65] *Ugt1a6* encodes UDP-glucuronosyltransferase, a key enzyme in the glucuronidation detoxification pathway.[66] Cellular stress response genes showed coordinated upregulation including *Clu*, which enhances HSF-1-mediated transcriptional activity and suppresses stress-induced apoptosis[67]; *Hspb7*, encodes a small heat-shock protein that helps cells handle stress by interacting with mechanosensitive proteins[68]; and *Ftl1*, encoding ferritin light chain that stores iron in a nontoxic state.[69] Genes related to mitochondrial functions that were upregulated included *Gba1*, which encodes β-glucocerebrosidase and plays a role in maintaining respiratory chain Complex I integrity and cellular energy homeostasis,[70] and *Kcng1*, a voltage-gated potassium channel regulating cellular excitability.[71] Conversely, the downregulated genes by ESW suggests a complex modulation of the cellular stress response, possibly involving alterations in chromatin structure (*Hist1h2an*),[72] immune regulation (*Slfn4, Il1rl1*),[73,74] protein synthesis (*Rpl22l1*),[75] and transcription (*Polr2k*)[76] in H9c2 cells.

The modulation of these genes may collectively enhance the cellular stress response following ESW treatment, potentially explaining the observed increase in cell viability and mitochondrial respiratory capacity under the oxidative stress state in H9c2 cells. In addition, the downregulation of *Ndufb1* (Complex I subunit)[77] and *Atp5mkl1* (ATP synthase component)[78] suggests a shift from oxidative phosphorylation to glycolysis, consistent with the observed increase in glycolytic ATP production in ESW-treated H9c2 cells. Overall gene expression profile suggests a shift towards a more resilient cellular state, better equipped to handle various stressors and maintain energy homeostasis.

Gene Ontology analysis predicted significant ESW-specific enrichment of biological processes related to the extracellular matrix (ECM), which regulates H9c2 cell behavior, differentiation, and function.[79] The upregulation of ECM-related processes may potentially improve the overall functional capacity and stress resistance of H9c2 cells in response to ESW treatment. In addition, increases in GO processes related to mechanical stress response, reactive oxygen species metabolism, glucose metabolism, and cellular stress responses suggest a comprehensive adaptation of H9c2 cells to manage stress-induced changes in their microenvironment and metabolic state. The modulation of these biological processes contributes to enhanced cellular resilience, improved energy metabolism, and increased capacity to withstand oxidative stress, ultimately leading to the observed increase in cell viability and

mitochondrial respiratory capacity in H9c2 cells.

Previous studies suggest that biological effects of structured water may depend on magnetic field intensity, exposure duration, and specific imprinting parameters. The variability in treatment parameters across studies may contribute to inconsistent findings in the literature.[4,15,16,80] While the present study demonstrates beneficial effects of ESW on H9c2 cells, several *in vivo* studies have reported null or adverse effects of structured water treatments.[4] Studies in lambs showed reduced food intake and depressed growth performance with electromagnetic water treatment,[4] while trials in broiler chickens reported no effects on growth or immune parameters.[4] These conflicting results may be due to rapid dilution within total body water and differences in water composition and treatment conditions, indicating that effects observed in controlled cellular studies may not necessarily translate to physiological benefits in whole organisms.[81] Like other complementary therapeutic interventions that target oxidative stress and metabolic pathways through exercise,[82] acupuncture,[83] and lifestyle modifications,[84] ESW may represent a novel approach to cellular stress management. However, unlike established interventions with demonstrated clinical efficacy,[83,85] the therapeutic potential of ESW requires validation through rigorous clinical trials.

The present study demonstrated that diluted ESW (10^{-2} and 10^{-3}) showed enhanced biological activity compared to higher concentrations (10^{-1}). This non-linear dose-response relationship may reflect hormetic effects where low doses produce optimal benefits while higher concentrations become inhibitory.[86] Additionally, dilution may optimize ionic strength and osmolarity for cellular compatibility, as salt concentration of undiluted ESW may create non-physiological conditions. The dilution process may alter water molecular cluster organization, creating configurations that interact more effectively with cellular membranes.[87] The observation that optimal activity occurs within a specific dilution range indicates that ESW's biological effects may depend on precise molecular interactions.

Several methodological limitations should be acknowledged. First, the use of immortalized H9c2 cells may not fully recapitulate primary cardiomyocyte responses, and the absence of *in vivo* validation limits translational interpretation of these cellular effects to the complex cardiovascular environment. This study did not assess physicochemical properties of ESW post-imprinting (pH, conductivity, surface tension, density, optical characteristics). This limitation highlights the need for future studies to systematically investigate optimal imprinting parameters, including magnetic field intensities, exposure duration, electromagnetic frequency combinations, and dose-response relationships. While these in-vitro findings suggest that ESW could potentially enhance cellular bioenergetics and stress resistance, validation through primary cardiomyocyte studies, comprehensive physicochemical characterization, and *in vivo* cardiac models are important before considering clinical applications.

Conclusion

In conclusion, the present study revealed that ESW plays a crucial role in cellular respiration and ATP synthesis, essential for cellular energy homeostasis. Our results indicate that ESW treatment protects H9c2 cells from oxidative stress-induced cytotoxicity by reducing ROS production. RNA-seq analysis revealed that ESW modulates the expression of genes related to stress response and energy metabolism in H9c2 cells. Notably, the enhanced biological activity observed at specific dilutions (10^{-2} and 10^{-3}) suggests that ESW effects may depend on optimal concentration ranges rather than maximum concentrations, indicating that water structural information can be preserved and potentially enhanced through appropriate dilution protocols. Understanding the influence of ESW on these cellular functions could provide new insights into optimizing cellular energy levels and overall metabolic efficiency. While this study highlights the potential health benefits of ESW, translating these findings to human applications will require extensive validation, including studies with primary cardiomyocytes, relevant animal models, characterizing ESW using NMR/FTIR spectroscopy to correlate structure and function, and ultimately clinical trials to establish efficacy and safety profiles.

List of abbreviations

ESW: Energized structured water, CW: Control water, ROS: Reactive oxygen species, DEGs: Differentially expressed genes, GO: Gene ontology, MTW: Magnetically treated water, ATP: Adenosine triphosphate, H_2O_2: Hydrogen peroxide, ECAR: Extracellular acidification rate, OCR: Oxygen consumption rate, FCCP: Carbonyl cyanide-p-trifluoromethoxyphenylhydrazone, Rot/AA: Rotenone and antimycin A, OXPHOS: Oxidative phosphorylation

Data availability statement

The RNA-seq datasets presented in this study can be found in the Gene Expression Omnibus (GEO) public repository (accession number GSE278403).

Funding

This work was supported by a Research Career Scientist Award from the Veterans Administration (BX005229).

CRediT authorship contribution statement

Sachithra S. Ranaweera: Writing – original draft, Visualization, Methodology, Investigation. **Juan P. Zuniga-Hertz:** Writing – review & editing, Supervision, Methodology. **Ramamurthy Chitteti:** Writing – review & editing, Methodology. **Andrei V. Chernov:** Writing – review & editing, Visualization, Software, Data curation. **Hemal H. Patel:** Writing – review & editing, Supervision, Funding acquisition, Conceptualization.

Acknowledgments

This publication includes data generated at the UC San Diego IGM Genomics Center utilizing an Illumina NovaSeq X Plus that was purchased with funding from a National Institutes of Health SIG grant (#S10 OD026929). HHP was supported by a Research Career Scientist Award from the Veterans Administration (BX005229).

Supplementary materials

Supplementary material associated with this article can be found, in the online version, at doi:10.1016/j.explore.2025.103232.

References

1. Wang Y, Wei H, Li Z. Effect of magnetic field on the physical properties of water. *Results Phys*. 2018;8:262–267.
2. Shafiei M, Ojaghlou N, Zamfir SG, Bratko D, Luzar A. Modulation of structure and dynamics of water under alternating electric field and the role of hydrogen bonding. *Mol Phys*. 2019;117(22):3282–3296.
3. DG E, Preparata G, Vitiello G. Water as a free electric dipole laser. *Phys Rev Lett*. 1988;61(9):1085–1088.
4. Lindinger MI. Structured water: effects on animals. *J Anim Sci*. 2021;99(5):1–11.
5. Moussa M, Zarai B, Hachicha M. Magnetic water treatment: theory and effects on treated water—a systematic review. *Euro-Mediterranean J Environ Integr*. 2025, 0123456789. https://doi.org/10.1007/s41207-024-00722-w. Available from.
6. Ramsey CL. Biologically Structured Water (BSW) - a Review (Part 1): structured Water (SW) Properties, BSW and redox biology, BSW and Bioenergetics. *J Basic Appl Sci*. 2023;19:174–201.
7. Abu-Saied MA, El Desouky EA, Abou Kamer ME, Hafez M, Rashad M. Influence of magnetic field on the physicochemical properties of water molecule under growing of cucumber plant in an arid region. *J King Saud Univ - Sci*. 2023;35(8), 102890. https://doi.org/10.1016/j.jksus.2023.102890. Available from:.
8. Smith CW. Quanta and Coherence Effects in Water and Living Systems. *J Altern Complement Med*. 2004;10(1):69–78. https://doi.org/10.1089/107555304322848977. Available from:.

9. Smith CW. Electromagnetic and magnetic vector potential bio-information and water. *Homeopathy*. 2015;104(4):301–304.
10. Gonet B. Influence of constant magnetic fields on certain physiochemical properties of water. *Bioelectromagnetics*. 1985;6(2):169–175.
11. Lednev VV. Possible mechanism for the influence of weak magnetic fields on biological systems. *Bioelectromagnetics*. 1991;12(2):71–75.
12. Ma YL, Ren H, Ren S, Zhen EK, Hao G, Zhao YW. A study of the effect of magnetized water on enzyme activities by potentiometric enzyme electrode method. *J Tongji Med Univ*. 1992;12(4):193–196.
13. Wu T, Brant JA. Magnetic Field Effects on pH and Electrical Conductivity: implications for Water and Wastewater Treatment. *Environ Eng Sci*. 2020;37(11):717–727.
14. Thomas Y. From high dilutions to digital biology: the physical nature of the biological signal. *Homeopathy*. 2015;104(4):295–300.
15. Ramsey CL. Application of a Structured Water Generator for Crop Irrigation: structured Water, Drought Tolerance, and Alteration of Plant Defense Mechanisms to Abiotic Stressors. *J Basic Appl Sci*. 2021;17.
16. Ali Ebrahim S. Biological Effects of Magnetic Water on Human and Animals. *Biomed Sci*. 2017;3(4):78.
17. Abd El-Ghany WA. Magnetized water as an alternative strategy to improve the poultry production system. *Iran J Vet Sci Technol*. 2022;14(3):1–10.
18. Alkudsi NH, Mazidawi HRH. Effect of magnatic water on milk production and its components in Holestein cows. *Iraqi J Vet Sci*. 2012;26(Suppl. IV):449–455.
19. Shamsaldain QZ, Al Rawee EA. Effect of magnetic water on productive efficiency of Awassi sheep. *Iraqi J Vet Sci [Internet]*. 2020;26:129–135. Available from: https://api.semanticscholar.org/CorpusID:131148392.
20. AH Al-Hilali. Effect of magnetically treated water on physiological and biochemical blood parameters of Japanese quail. *Int J Poult Sci*. 2018;17(2):78–84.
21. Lee HJ, Kang MH. Effect of the magnetized water supplementation on blood glucose, lymphocyte DNA damage, antioxidant status, and lipid profiles in STZ-induced rats. *Nutr Res Pr*. 2013;7(1):34–42. https://doi.org/10.4162/nrp.2013.7.1.34. Available from:.
22. Hwang SG, Lee HS, Lee BC, Bahng GW. Effect of Antioxidant Water on the Bioactivities of Cells. *Int J Cell Biol*. 2017:2017.
23. Minoretti P, A Santiago Sáez, M Liaño Riera, M Gómez Serrano, Á García Martín. Topically Applied Magnetized Saline Water Improves Skin Biophysical Parameters Through Autophagy Activation: a Pilot Study. *Cureus*. 2023;15(11), e49180.
24. Brizzi EV Di, Lista S, García-chico C., Khoramipour K., Santos-lozano A., Minoretti P. Smart Fluids As Autophagy-Activating Photoprotectors : in Vitro Analysis of Dead Sea Water and Magnetized Saline Water Against Ultraviolet B (UVB) -Induced Photodamage in Human Keratinocytes. 2025;17(4).
25. Kuznetsov AV, Javadov S, Sickinger S, Frotschnig S, Grimm M. H9c2 and HL-1 cells demonstrate distinct features of energy metabolism, mitochondrial function and sensitivity to hypoxia-reoxygenation. *Biochim Biophys Acta*. 2015 Feb;1853(2):276–284.
26. Peter H, Fraser HM. *Decoding the Human Body-Field The New Science of Information as Medicine*. Rochester, Vermont: Healing Arts Press; 2008.
27. Bai J, Liu Z, Liu J, Zhang S, Tian Y, Zhang Y, et al. Mitochondrial metabolic study guided by proteomics analysis in hepatocellular carcinoma cells surviving long-term incubation with the highest dose of sorafenib. *Aging (Albany NY)*. 2019;11(24):12452–12475.
28. Chen S, Zhou Y, Chen Y, Gu J. fastp: an ultra-fast all-in-one FASTQ preprocessor. *Bioinformatics*. 2018;34(17):i884–i890.
29. Patro R, Duggal G, Love MI, Irizarry RA, Kingsford C. Salmon provides fast and bias-aware quantification of transcript expression. *Nat Methods*. 2017;14(4):417–419.
30. Ewels P, Magnusson M, Lundin S, Käller M. MultiQC: summarize analysis results for multiple tools and samples in a single report. *Bioinformatics*. 2016;32(19):3047–3048.
31. Love MI, Soneson C, Hickey PF, Johnson LK, Pierce NT, Shepherd L, et al. Tximeta: reference sequence checksums for provenance identification in RNA-seq. *PLoS Comput Biol*. 2020 Feb;16(2), e1007664.
32. Love MI, Huber W, Anders S. Moderated estimation of fold change and dispersion for RNA-seq data with DESeq2. *Genome Biol*. 2014;15(12):550.
33. Stephens M. False discovery rates: a new deal. *Biostatistics*. 2017;18(2):275–294.
34. Ritchie ME, Phipson B, Wu D, Hu Y, Law CW, Shi W, et al. limma powers differential expression analyses for RNA-sequencing and microarray studies. *Nucleic Acids Res*. 2015;43(7):e47.
35. Risso D, Ngai J, Speed TP, Dudoit S. Normalization of RNA-seq data using factor analysis of control genes or samples. *Nat Biotechnol*. 2014 Sep;32(9):896–902.
36. Wu T, Hu E, Xu S, Chen M, Guo P, Dai Z, et al. clusterProfiler 4.0: a universal enrichment tool for interpreting omics data. *Innov (Camb)*. 2021;2(3), 100141.
37. Kanehisa M, Furumichi M, Sato Y, Kawashima M, Ishiguro-Watanabe M. KEGG for taxonomy-based analysis of pathways and genomes. *Nucleic Acids Res*. 2023;51(D1):D587–D592.
38. Ashburner M, Ball CA, Blake JA, Botstein D, Butler H, Cherry JM, et al. Gene ontology: tool for the unification of biology. The Gene Ontology Consortium. *Nat Genet*. 2000;25(1):25–29.
39. Gentleman R, Carey V, Bates D, Bolstad B, Dettling M, Dudoit S, et al. Bioconductor: open software development for computational biology and bioinformatics. *Genome Biol*. 2004;5(10):R80.
40. Shannon P, Markiel A, Ozier O, Baliga NS, Wang JT, Ramage D, et al. Cytoscape: a software environment for integrated models of biomolecular interaction networks. *Genome Res*. 2003;13(11):2498–2504.
41. Otasek D, Morris JH, Bouças J, Pico AR, Demchak B. Cytoscape Automation: empowering workflow-based network analysis. *Genome Biol*. 2019;20(1):185.
42. Gu X, Ma Y, Liu Y, Wan Q. Measurement of mitochondrial respiration in adherent cells by Seahorse XF96 Cell Mito Stress Test. *STAR Protoc*. 2021;2(1), 100245. Available from: https://www.sciencedirect.com/science/article/pii/S266616672030232X.
43. Jang DH, Greenwood JC, Spyres MB, Eckmann DM. Measurement of Mitochondrial Respiration and Motility in Acute Care: sepsis, Trauma, and Poisoning. *J Intensive Care Med*. 2017;32(1):86–94.
44. Marchetti P, Fovez Q, Germain N, Khamari R, Kluza J. Mitochondrial spare respiratory capacity: mechanisms, regulation, and significance in non-transformed and cancer cells. *FASEB J*. 2020;34(10):13106–13124. https://doi.org/10.1096/fj.202000767R. Available from:.
45. Desler C, Hansen TL, Frederiksen JB, Marcker ML, Singh KK. Juel Rasmussen L. Is There a Link between Mitochondrial Reserve Respiratory Capacity and Aging? *J Aging Res*. 2012;2012, 192503.
46. Sansbury BE, Jones SP, Riggs DW, Darley-Usmar VM, Hill BG. Bioenergetic function in cardiovascular cells: the importance of the reserve capacity and its biological regulation. *Chem Biol Interact*. 2011;191(1–3):288–295.
47. Chen S, Zou Y, Song C, Cao K, Cai K, Wu Y, et al. The role of glycolytic metabolic pathways in cardiovascular disease and potential therapeutic approaches. *Basic Res Cardiol*. 2023;118(1):48.
48. Lopaschuk GD, Karwi QG, Tian R, Wende AR, Abel ED. Cardiac Energy Metabolism in Heart Failure. *Circ Res*. 2021;128(10):1487–1513.
49. Hargreaves M, Spriet LL. Skeletal muscle energy metabolism during exercise. *Nat Metab*. 2020;2(9):817–828. https://doi.org/10.1038/s42255-020-0251-4. Available from:.
50. Karwi QG, Uddin GM, Ho KL, Lopaschuk GD. Loss of Metabolic Flexibility in the Failing Heart. *Front Cardiovasc Med*. 2018;5:1–19.
51. Flood D, Lee ES, Taylor CT. Intracellular energy production and distribution in hypoxia. *J Biol Chem*. 2023;299(9), 105103.
52. Pollack G.H. The Fourth Phase of Water: Beyond Solid, Liquid, and Vapor. Ebner & Sons Publishers, Seattle, WA. 357 pages. ISBN: 978-0-9626895-4-3.
53. Lang X, Shi L, Zhao Z, Min W. Probing the structure of water in individual living cells. *Nat Commun*. 2024;15(1):5271. https://doi.org/10.1038/s41467-024-49404-9. Available from:.
54. Ho MW. Illuminating water and life: emilio Del Giudice. *Electromagn Biol Med*. 2015;34(2):113–122.
55. Geesink HJH, Jerman I, Water Meijer DKF. The Cradle of Life via its Coherent Quantum Frequencies. *Water*. 2020;11:78.
56. Moris D, Spartalis M, Tzatzaki E, Spartalis E, Karachaliou GS, Triantafyllis AS, et al. The role of reactive oxygen species in myocardial redox signaling and regulation. *Ann Transl Med*. 2017;5(16):324.
57. Jang MH, Piao XL, Kim JM, Kwon SW, Park JH. Inhibition of cholinesterase and amyloid-&bgr; aggregation by resveratrol oligomers from Vitis amurensis. *Phyther Res*. 2008;22(4):544–549. Available from: http://www3.interscience.wiley.com/journal/117934759/abstract.
58. Jin M, Yu H, Jin X, Yan L, Wang J, Wang Z. Dracocephalum moldavica L. Extracts Protect H9c2 Cardiomyocytes against H2O2-Induced Apoptosis and Oxidative Stress. *Biomed Res Int*. 2020;2020.
59. Devkar RV, Pandya AV, Shah NH. Protective role of Brassica olerecea and Eugenia jambolana extracts against H2O2 induced cytotoxicity in H9C2 cells. *Food Funct*. 2012;3(8):837–843.
60. Zhang L, Liu Y, Li JY, Li LZ, Zhang YL, Gong HY, et al. Protective Effect of Rosamultin against H2O2 -Induced Oxidative Stress and Apoptosis in H9c2 Cardiomyocytes. *Oxid Med Cell Longev*. 2018;2018.
61. Sun X, Sun GB, Wang M, Xiao J, Sun XB. Protective effects of cynaroside against H2O2-induced apoptosis in H9c2 cardiomyoblasts. *J Cell Biochem*. 2011;112(8):2019–2029.
62. Burghardt TP, Neff KL, Wieben ED, Ajtai K. Myosin individualized: single nucleotide polymorphisms in energy transduction. *BMC Genomics*. 2010;11(1):172. https://doi.org/10.1186/1471-2164-11-172. Available from:.
63. Taverna S, Cammarata G, Colomba P, Sciarrino S, Zizzo C, Francofonte D, et al. Pompe disease: pathogenesis, molecular genetics and diagnosis. *Aging (Albany NY)*. 2020;12(15):15856–15874.
64. Tang Z, Xia C, Huang R, Li X, Wang WC, Guo W, et al. Aldo-keto reductase family 1 member B8 is secreted via non-classical pathway. *Int J Clin Exp Pathol*. 2014;7(7):3791–3799.
65. Sebastián VP, Salazar GA, Coronado-Arrázola I, Schultz BM, Vallejos OP, Berkowitz L, et al. Heme Oxygenase-1 as a Modulator of Intestinal Inflammation Development and Progression. *Front Immunol*. 2018;9. Available from: https://www.frontiersin.org/journals/immunology/articles/10.3389/fimmu.2018.01956.
66. Meech R, Hu DG, McKinnon RA, Mubarokah SN, Haines AZ, Nair PC, et al. The UDP-Glycosyltransferase (UGT) Superfamily: new Members, New Functions, and Novel Paradigms. *Physiol Rev*. 2019;99(2):1153–1222. https://doi.org/10.1152/physrev.00058.2017. Available from:.
67. Gross C, Guérin LP, Socol BG, Germain L, Guérin SL. The Ins and Outs of Clusterin: its Role in Cancer, Eye Diseases and Wound Healing. *Int J Mol Sci*. 2023;24.
68. Collier MP, Benesch JLP. Small heat-shock proteins and their role in mechanical stress. *Cell Stress Chaperones*. 2020 Jul;25(4):601–613.
69. Li W, Garringer HJ, Goodwin CB, Richine B, Acton A, VanDuyn N, et al. Systemic and cerebral iron homeostasis in ferritin knock-out mice. *PLoS One*. 2015;10(1), e0117435.
70. Baden P, Perez MJ, Raji H, Bertoli F, Kalb S, Illescas M, et al. Glucocerebrosidase is imported into mitochondria and preserves complex I integrity and energy metabolism. *Nat Commun*. 2023;14(1):1930. https://doi.org/10.1038/s41467-023-37454-4. Available from:.

71. Nerbonne JM, Nichols CG, Schwarz TL, Escande D. Genetic manipulation of cardiac K(+) channel function in mice: what have we learned, and where do we go from here? *Circ Res*. 2001;89(11):944–956.
72. Bönisch C, Hake SB. Histone H2A variants in nucleosomes and chromatin: more or less stable? *Nucleic Acids Res*. 2012;40(21):10719–10741.
73. Akhabir L, Sandford A. Genetics of interleukin 1 receptor-like 1 in immune and inflammatory diseases. *Curr Genomics*. 2010;11(8):591–606.
74. van Zuylen WJ, Garceau V, Idris A, Schroder K, Irvine KM, Lattin JE, et al. Macrophage activation and differentiation signals regulate schlafen-4 gene expression: evidence for Schlafen-4 as a modulator of myelopoiesis. *PLoS One*. 2011; 6(1), e15723.
75. O'Leary MN, Schreiber KH, Zhang Y, Duc ACE, Rao S, Hale JS, et al. The Ribosomal Protein Rpl22 Controls Ribosome Composition by Directly Repressing Expression of Its Own Paralog, Rpl22l1. *PLOS Genet*. 2013;9(8), e1003708. https://doi.org/10.1371/journal.pgen.1003708. Available from:.
76. Muste Sadurni M, Saponaro M. Deregulations of RNA Pol II Subunits in Cancer. *Applied Biosciences*. 2023;2(3):459–476, 2.
77. Zhang R, Hou T, Cheng H, Wang X. NDUFAB1 protects against obesity and insulin resistance by enhancing mitochondrial metabolism. *FASEB J Off Publ Fed Am Soc Exp Biol*. 2019;33(12):13310–13322.
78. Galber C, Carissimi S, Baracca A, Giorgio V. The ATP Synthase Deficiency in Human Diseases. *Life (Basel)*. 2021 Apr;11(4).
79. Suhaeri M, Subbiah R, SY Van, Du P, Kim IG, Lee K, et al. Cardiomyoblast (h9c2) differentiation on tunable extracellular matrix microenvironment. *Tissue Eng Part A*. 2015;21(11–12):1940–1951.
80. Fujimura Y, Iino M. Magnetic field increases the surface tension of water. *J Phys Conf Ser*. 2009;156, 012028.
81. Chibowski E, Szcześ A. Magnetic water treatment–a review of the latest approaches. *Chemosphere*. 2018;203:54–67. Available from: https://www.sciencedirect.com/science/article/pii/S0045653518305836.
82. Mohamed A., Ismail A., Morsy M.M., Saber O., Saber A., Mohamed A., et al. Comparative response of oxidative stress to baduanjin exercise versus electro-acupuncture in patients with type 2 diabetes mellitus. 2025;13(3):599–606.
83. Ismail AMA, Alahmari M, Elsisi HF, Ghaleb HAM. Effect of adding pranayama yoga exercises to laser acupuncture on inflammatory markers in elderly with allergic rhinitis: a randomized controlled study. *Electron J Gen Med*. 2025;22(3).
84. Ismail AMA, El-Azeim ASA, Saif HFAEA. Effect of aerobic exercise alone or combined with Mediterranean diet on dry eye in obese hypertensive elderly. *Ir J Med Sci*. 2023 Dec;192(6):3151–3161.
85. Ismail AMA, Abd Elfatah Abo Saif HF, El-Moatasem Mohamed AM. Effect of Jyoti-Trataka on intraocular pressure, autonomic control, and blood glucose in diabetic patients with high-tension primary open-angle glaucoma: a randomized-controlled trial. *J Complement Integr Med*. 2022 Dec;19(4):1013–1018.
86. Calabrese EJ, Baldwin LA. Hormesis: the dose-response revolution. *Annu Rev Pharmacol Toxicol*. 2003;43:175–197.
87. Elia V, Germano R, Napoli E. Permanent dissipative structures in water: the matrix of life? Experimental evidences and their quantum origin. *Curr Top Med Chem*. 2015; 15(6):559–571.